Kingdom of Saudi Arabia
Imam Mohammad Ibn Saud Islamic University (IMSIU)
Faculty of Sciences – Department of Physics

Geant4 Study of Electron Deflection in a Magnetic Field for Electron Therapy Beam Profiling

A graduation project submitted to the Department of Physics in partial fulfillment of the requirements for the degree of Bachelor of Science in Applied Physics

By

Joud Aleready

Nujum Majrabi

Supervisor/s

Dr. Hanan Akhdr

Dr. Maha Algarawi

IMSIU-Riyadh-KSA

May , 2025


بسم الله الرحمن الرحيم

Acknowledgements

I extend my heartfelt gratitude to Allah, the Almighty, for granting me the strength and guidance to complete this research successfully. I am deeply indebted to my supervisors, Dr.Hanan Akhdr Dr.Maha Algarawi, for her invaluable guidance, encouragement, and constructive feedback throughout this project. Her expertise and support have been instrumental in the completion of this thesis. I would also like to express my appreciation to the faculty members of the Department of Physics at Imam Muhammad Ibn Saud Islamic University for their continuous support and for providing the necessary resources to carry out this study.

Table of Contents

List of Tables

List of Figures

الملخص

يهدف هذا المشروع إلى تطوير نموذج محاكاة باستخدام Geant4، يحلل تأثير المجالات المغناطيسية على مسارات الإلكترونات والجسيمات المشحونة الأخرى في علم الأورام بالأشعة. يركز البحث على تحديد زوايا الانحراف وتقييم طريقة ترسب الطاقة داخل الورم مقارنةً بالأنسجة خارج الهدف. الهدف الرئيسي هو تحسين دقة توصيل حزمة الإشعاع، وتقليل الضرر الذي يلحق بالأنسجة السليمة، وتطوير بروتوكولات علاجية أكثر أمانًا وفعالية.

Abstract

The purpose of the project is to develop a simulation model with Geant4, which analyzes the effect of magnetic fields on electron's and other charged particle's trajectories in radiography oncology. The investigation focuses on determining deflection angles and assessing the way in which energy is deposited inside the tumor compared to tissues outside the target. The main purpose is to improve the accuracy of the radiation beam delivery, minimize damage to healthy tissue, and further develop safer and more effective protocols that incorporate treatment.

Chapter 1: Introduction

In recent decades, the increasing incidence of cancer and the limitations of conventional treatments, such as chemotherapy, have underscored the need for more precise and effective therapeutic approaches. One of the most significant advancements in cancer treatment is the use of electron and proton beam therapy, which allows for targeted radiation delivery while minimizing damage to surrounding healthy tissues. However, precise control of electron beam deflection is critical for optimizing dose distribution and ensuring effective tumor targeting [1].

To achieve this, advanced magnetic beam steering systems are required to manipulate electron trajectories accurately. Simulation techniques, particularly Monte Carlo-based models, play a crucial role in analyzing and optimizing these systems to enhance treatment efficacy [2].

1.1 MRI-Guided Radiation Therapy and electron beams

The integration of electron beams into MRgRT enables improved accuracy and extends the capabilities of this technologically advanced treatment approach.

Modern radiation therapy aims to maximize tumor dose delivery while minimizing healthy tissue exposure. The development of MRI-guided radiation therapy (MRgRT) has revolutionized treatment precision by enabling real-time imaging and adaptive radiation delivery. Most MRI-linear Accelerator systems focus on photon-based radiation therapy, but the integration of electron beams in MRI-linear accelerator systems remains an open area of research [1].

This study explores the behavior of electron beams in the presence of magnetic fields comparable to those in MRI-linear accelerator systems. Using a combination of experimental measurements and Monte Carlo simulations (Geant4), the study evaluates potential improvements in dose distribution under transverse and inline magnetic field configurations [1].

1.2 Radiation therapy and cancer

More than 50% of all cancer patients require radiotherapy as part of their treatment. Although photons have historically been the primary modality for radiation therapy [3] , electrons are preferred in certain cases due to their physical properties, particularly their limited penetration depth in tissue [4].

For treating tumors which appear near or directly on the skin surface the therapy with electron beams provides specific advantages. The rapid dose reduction of electron beams makes them suitable for treating superficial tumors because it protects deeper healthy tissues. This treatment property allows electrons to function best when treating skin surface tumors[5].

1.3 Magnetic field role in electron therapy

Magnetic field implementations in electron beam therapy use affected charged particles' pathways to improve dose delivery accuracy. The Geant4 simulation models show magnetic fields redirect electron paths to improve target area dose conformity while protecting surrounding healthy tissues from exposure [6].

These conditions were achieved by irradiating the cells at different depths in water using nominal electron beams.

Electron therapy offers better dose distribution than X-ray, minimizing damage to normal tissues. Tumor cells are more vulnerable to electron irradiation due to differences in repair capacity. A new fractionation schedule, developed by Schumacher in Berlin, uses higher doses once a week, effectively reducing tumor cells while protecting normal cells. This method also promotes rexygenation of anoxic tumor cells. Clinical results from 4,262 cases show significant improvement with this approach [4].

1.4 Radiation Interaction with Matter

The interaction between matter and radiation differs greatly depending on the type of radiation concerned. Photon energy is the main factor determining the dominant microscopic interaction mechanisms for such kinds of electromagnetic radiation as gamma rays and X-rays. At lower energies the photoelectric effect prevails, when the photon hands over all its energy to an atomic electron. When energy of photons increases, then Compton scattering emerges as dominant mechanism, where there is various energy exchange (partially) and bending of photon. At even

higher energies (above 1.022MeV), pair production is seen with the generation of an electron-positron pair. Macroscopically the intensity of electromagnetic radiation usually drops exponentially with the material thickness according to the thinned-film laser absorption by the Beer–Lambert law [8].

In contrast, particle radiation (e.g., electrons, protons, neutrons) interacts with matter on the basis of mass and electric charge of the particle being considered. The cost of charged particles (positive or negative) favors Columbic interactions whereby the particle gets deflected due to electromagnetic force from atomic nuclei or electrons. Collisions directly may take place, but their probability, statistically, is lower. Neutral neutrons mostly react through nuclear collisions or capture and as such cause secondary radiation or nuclear reaction [8].
These interaction mechanisms are highly important in medical physics; radiation protection and material analysis; and form the basis for technologies like radiation therapy, diagnostic imaging and shielding design [8].

1.5 Simulation

Modeling a real system into a representation allows researchers to conduct experiments either for behavioral analysis or operational strategy evaluation [7].
Monte Carlo codes for radiation therapy:
• Several well-established Monte Carlo simulation packages exist, including EGSnrc, GEANT4, MCNP6, and PENELOPE.
• GEANT4 was selected for this study due to its straightforward implementation of magnetic fields, ease of handling non-uniform fields, and general usability [2].
• Monte Carlo simulations are invaluable for validating treatment plans, investigating new radiation techniques, and optimizing treatment delivery methods [4].

1.6 Aim of this work

This work aims to evaluate the influence of magnetic fields on electron beam trajectories to optimize electron therapy. The study focuses on assessing changes in deflection angle due to uniform magnetic fields, and analyzing energy deposition in pre-tumor, tumor, and post-tumor regions to identify optimal treatment parameters.

Chapter 2: Materials & Methods

The interaction between charged particles and electromagnetic fields is a cornerstone of classical and modern physics, with applications ranging from particle accelerators to medical radiation therapy. Central to this interaction is the Lorentz force, which describes how a charged particle is influenced by electric and magnetic fields. When moving through a magnetic field, a charged particle experiences a perpendicular force that alters its path, often resulting in circular motion. The nature of this motion is governed by the particle's charge, mass, velocity, and the strength and orientation of the magnetic field.

To analyze and simulate these complex interactions, computational tools such as Geant4 are employed. Geant4 is a powerful simulation toolkit that enables detailed modeling of particle interactions with matter, incorporating both electromagnetic and hadronic processes. This study focuses on exploring the motion of charged particles under magnetic fields, understanding the factors that affect their angle of deflection, and validating simulation results using Geant4. By comparing analytical calculations with simulated data across various particle types and energy levels, the research aims to ensure the accuracy and reliability of simulations used in experimental and applied physics.

2.1 Lorentz force and charged particle motion

- Magnetic Force on a Charged Particle

The magnetic force acting on a charged particle exists perpendicularly to the magnetic field according to the expression:

$$F = qvB \qquad (2.1)$$

where q is the charge of the particle, B is the magnetic field vector, v is the velocity of the particle.

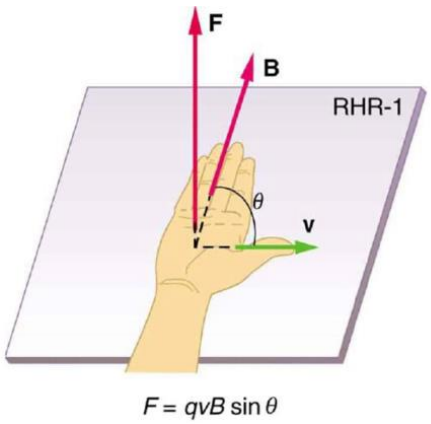

Figure 2.1: Right hand rule directions.

Right Hand Rule: Magnetic fields exert forces on moving charges. This The direction of the magnetic force on a moving charge is perpendicular to the plane formed by v and B and follows right hand rule as shown figure 2.2 the magnitude of the force is proportional to $q, v\,.B$ according to the expression:

$$F = qvB\sin\theta \qquad (2.2)$$

This force acts as the centripetal force that keeps the particle in circular motion. Setting the magnetic force equal to the centripetal force:

$$qvB = \frac{mv^2}{r} \qquad (2.3)$$

Where m is the mass of the particle, r is the radius of the circular path. If the particle velocity happens to be aligned parallel to the magnetic field, or is zero, the magnetic force will be zero [8].

- Lorentz Force

The Lorentz force is the combined force on a charged particle due both electric and magnetic fields, which are often considered together for practical applications. If a particle of charge q moves with velocity v in the presence of an electric field E and a magnetic field B, then it will experience a force Lorentz [9]:

where E is the electric field vector , B is the magnetic field vector

$$F = q(E + v * B) \qquad (2.4)$$

With no electric field, this simplifies to:

$$F = (qvB) \qquad (2.5)$$

2.2 Angle of deflection

The angle dependence of the magnetic field also causes charged particles to move perpendicular to the magnetic field lines in a circular or helical fashion, while a particle in an electric field will move in a straight line along an electric field line.

This represents the angle θ (in radians) swept by a charged particle moving in a magnetic field over a path length L.

$$\theta = \frac{L}{r} \qquad (2.6)$$

$$\theta = \frac{qBL}{mv} \qquad (2.7)$$

where θ is the angle (in radians) that is the particle sweeps along its circular path, L is the arc length or distance the particle travels along is the curved path , r is the radius of the circular path , q is the charge of the particle , B is the magnetic field strength , m is the mass of the particle ,v is the speed of the particle perpendicular to the magnetic field.

Equation (2.6) comes from the basic geometry of a circle, where the angle in radians equals arc length divided by the radius , equation (2.7) results from substituting the expression for the radius r (from equating magnetic force to centripetal force) into the (2.6) equation. So this equation connects the angular displacement of a particle with its physical properties and the magnetic field it's moving through.

2.3 Geant4

Geant4 is a toolkit designed for simulating the transport of radiation through matter. With its flexible core and a variety of physics modeling options, it caters to a wide range of applications [10].

The toolkit allows users to define the geometry and materials of a setup or detector, navigate within it, simulate physical interactions using different physics engines and cross-section models, and visualize and store results [10].

It provides physics models that describe electromagnetic and hadronic interaction, as well as processes like decays and interaction of optical photons. Several models with varying levels of precision and performance are available to suit different processes. The toolkit includes pre-configured physics setups known as physics lists, which users can either adopt or customize based on their specific requirements and applications areas. Its clear structure and readable code enable users to explore the origins of physics results effectively [10].

Applications areas include detector simulation and background studies in high-energy physics experiments, accelerator setup simulations, medical imaging, and radiation therapy studies, and investigating the effects of solar radiation on spacecraft instruments [10].

2.3.1 Validation of the Geant4

The Geant4 simulation contained an implemented uniform magnetic field which analyzed the response of charged electrons' deflection due to a magnetic field to different energy .

The simulation generated momentum vector information that researchers used to perform manual calculations of deflection angles. Compared outputs of manually determined angles with Geant4 direct values for checking simulation result precision and reliability.

The magnetic field is oriented along the Y-axis, and the electron is emitted perpendicular to the Z-axis.

Due to its small mass, the electron is strongly affected by the magnetic field, causing it to move in a circular path around the magnetic field lines, potentially completing multiple rotations.

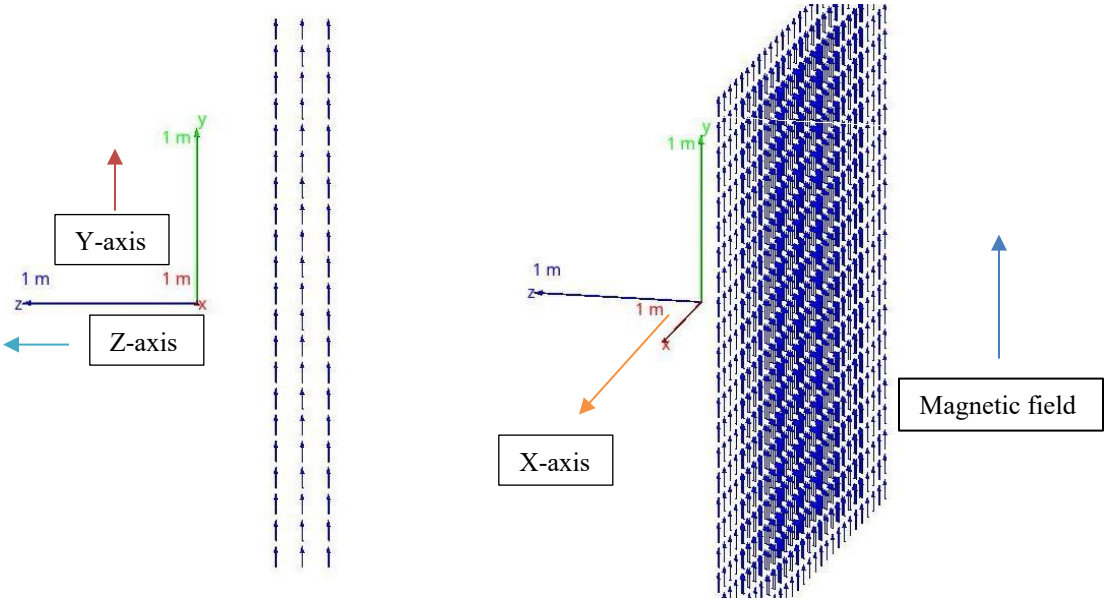

Figure 2.2:Magnetic field direction with axes in air.

Figure 2.2 shows (right) depict a uniform magnetic field that's directed upwards along the y-axis. In (left) the magnetic field is confined to a small area.

it's apparent in the figure 2.2 shows (right) that the field occupies a much larger region in space. This rotational motion increases the likelihood of errors in measurements or simulations.

To reduce these errors, heavier particles—such as protons or heavy ions-are used, as they are less influenced by the magnetic field and exhibit more stable trajectories.

The method used to find the deflection angle in the Geant4 simulation, the principle of momentum conservation is employed by calculating the initial momentum of a charged particle before entering the magnetic field and its final momentum after exiting. The deflection angle is then determined by computing the dot product of the initial and final momentum vectors using the following expression:

$$Cos(\theta) = \frac{\vec{P}_i \bullet \vec{P}_f}{|\vec{P}_i||\vec{P}_f|} \qquad (2.8)$$

2.3.2 Validation in Geant4 for different particles

Geant4 software produced a simulated model of a water phantom that included a tumor. The research team tested different magnetic field powers and particle energy levels through their simulations which ran on shallow and deep water models to discover an optimal treatment combination for tumors .

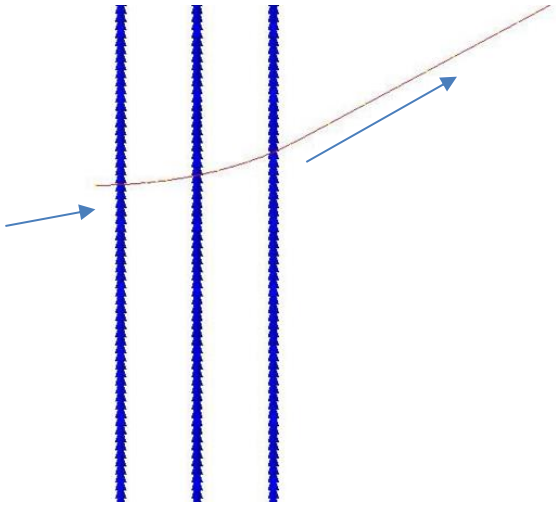

Figure 2.3: Electron in air.

Figure 2.4 shows after zipping almost straight, the electron follows a slightly upward path when passing through the blue lines. Therefore, the moving electron was affected by the air a bit and shifted its direction.

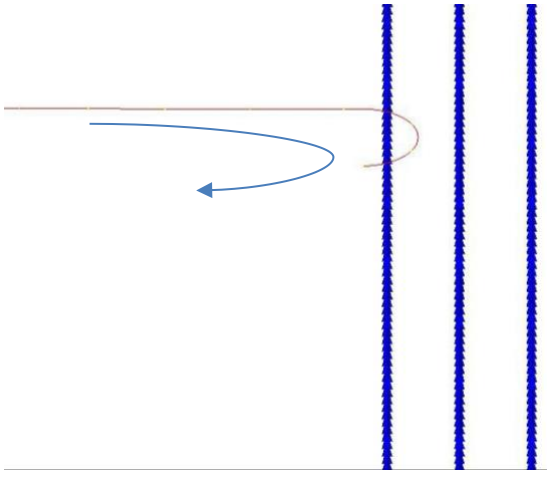

Figure 2.5: Electron collision and reflection in air .

Figure 2.6 shows electron moves straight, but as soon as it gets to one of the blue lines, it changes directions and goes back in the other direction. This means that the electron hit something really hard at that point, which made it change its direction quickly.

To determine the velocity of the particle, we employed the relativistic energy-momentum relationship, as we are dealing with subatomic particles—specifically, electrons. In this context, relativistic effects become significant due to the high velocities involved. As a result, classical mechanics is insufficient for accurately describing their behavior. Therefore, we use the following equation derived from special relativity:

$$v = c\sqrt{1 - (\frac{mc^2}{E})^2} \qquad (2.9)$$

where v is velocity of particle , c is speed of light, m is mass of particle, E is total energy.

The objective of the validation process in the Geant4 code is to ensure accurate and efficient execution of simulations, particularly in calculating the deflection angle both through Geant4 and analytical methods. The percentage error is then determined by comparing the simulated results with the theoretical or manually calculated values, using the following relation:

$$\text{Error precentage } \% = \frac{\text{simulated value} - \text{calculated value}}{\text{calculated value}} \times 100$$

We calculated the error percentage as shown below:

Electron Data

Table 2.1: Validation in Geant4 for electron particle

Magnetic Field (T)	**Energy (MeV)**	**Speed (m/s)**	**Length (m)**	**Angle (radian)**	**Angle (degree)**	**Simulation**	**Error (%)**
0.05	20	2.99907E+08	0.4	672.029	38504.42	17.2321	99.95525
0.05	30	2.99958E+08	0.4	671.914	38497.85	11.1988	99.97091
0.06	20	2.99907E+08	0.4	806.435	46205.3	20.6721	99.95526
0.06	30	2.99072E+08	0.4	808.685	46334.21	179.893	99.61175
0.08	20	2.99907E+08	0.4	18.7666	1075.25	27.8568	97.40926
0.08	30	2.99958E+08	0.4	1075.06	61596.56	18.5238	99.96993

The mass of e^- is very light that make it move circular motion becomes tighter (with smaller radius). Sometimes, a particle travels several times inside a loop before exiting and Geant4 uses its emission and final momentum to calculate its angle.

Proton Data

Table 2.2: Validation in Geant4 for proton particle

Magnetic Field (T)	Energy (MeV)	Speed (m/s)	Length (m)	Angle (radian)	Angle (degree)	Simulation	Error (%)
0.5	250	1.84E+08	0.4	0.104	5.96	4.68504	21.4469
0.5	200	1.70E+08	0.4	0.113	6.46	5.30209	17.97835
0.6	250	1.84E+08	0.4	0.125	7.16	5.62433	21.41502
0.6	200	1.70E+08	0.4	0.135	7.76	6.36581	17.93578

Alpha Particle Data

Table 2.3: Validation in Geant4 for alpha particle

Magnetic Field (T)	Energy (MeV)	Speed (m/s)	Length (m)	Angle (radian)	Angle (degree)	Simulation	Error (%)
0.5	100	6.81E+07	0.4	0.142	8.12	7.86435	3.10316
0.5	200	9.45E+07	0.4	0.102	5.85	7.38004	26.14929
0.8	100	6.81E+07	0.4	0.227	12.99	12.5841	3.094381
0.8	200	9.45E+07	0.4	0.163	9.36	8.84376	5.519306

In contrast, simulations involving heavier particles such as protons and alpha particles demonstrate much greater accuracy, as seen in tables 2.4 and 2.5 the higher mass of these particles results in reduced sensitivity to magnetic fields, leading to more stable trajectories and smaller deviations between simulated and theoretical values. This makes heavier particles more suitable.

Chapter 3: Result

3.1 Water phantom

We have two levels in the case of the water phantom medium to see in which cases it is better for electron therapy A deep level and shallow.

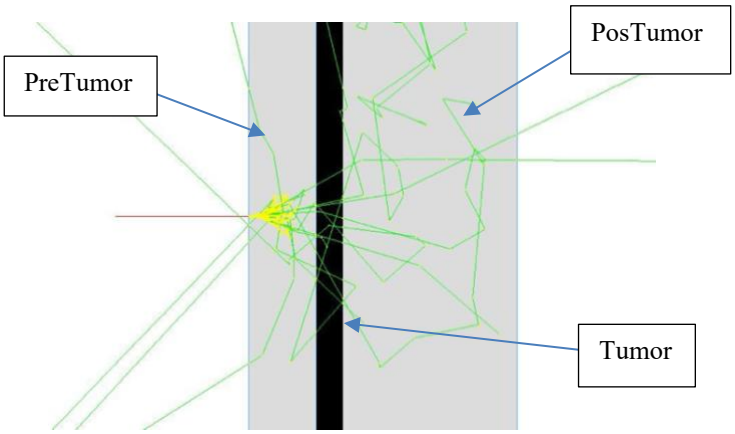

Figure 3.1: Electron direction in water phantom.

The path of electrons change randomly as they interact with objects in the phantom.

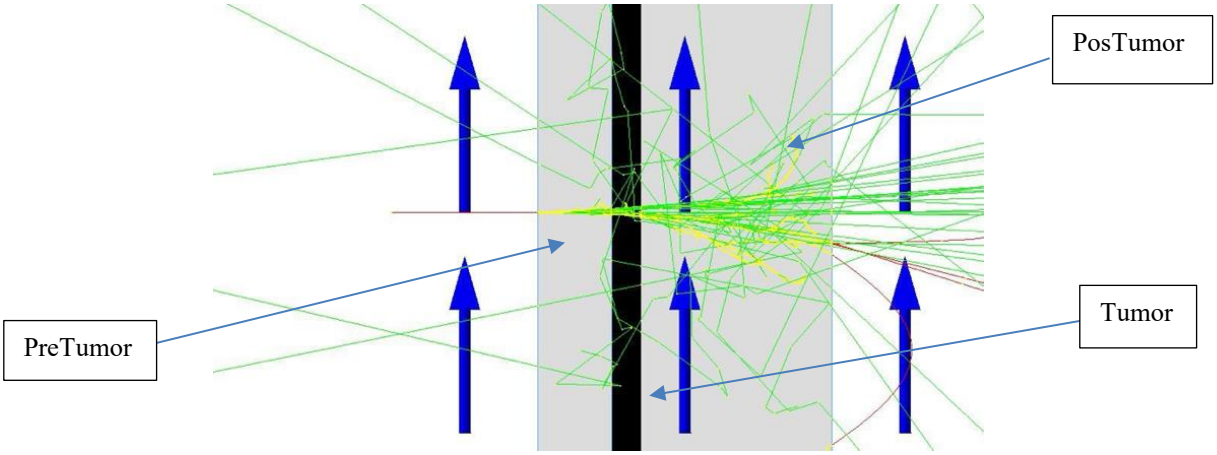

Figure 3.2: Electron with phantom with direction of magnetic field.

When electrons follow more organized paths, the beam can be directed and the amount of energy used can be controlled better. Different energy levels were tested on both deep and shallow tumors in the presence of a constant magnetic field as shown in figure 3.2.

Deep level:

In electron beam radiation therapy, the deep dose means the level of radiation that gets into tissues deeper than the surface and the depth of maximum dose.

Different energy levels were tested on both deep and shallow tumors in the presence of a constant magnetic field.

Table 3.1: Geant4-Simulated deflection of 10-electron beam in deep tumor under 0.04 T magnetic field at various energies.

Magnetic Field (T)	Energy (MeV)	PreTumor	Tumor	PostTumor	θMean (degree)	θStd.Dev (degree)	Tumor %
0.04	15	19.9381	8.82946	0.142629	0.00902928	1.06926	30.54099716
0.04	16	20.9435	10.8248	1.53158	0.00734656	0.801553	32.50702405
0.04	17	20.8152	10.4715	3.27925	0.00928105	1.15873	30.29426357
0.04	18	11.0034	11.0034	3.42721	0.00948809	1.00918	43.26254492

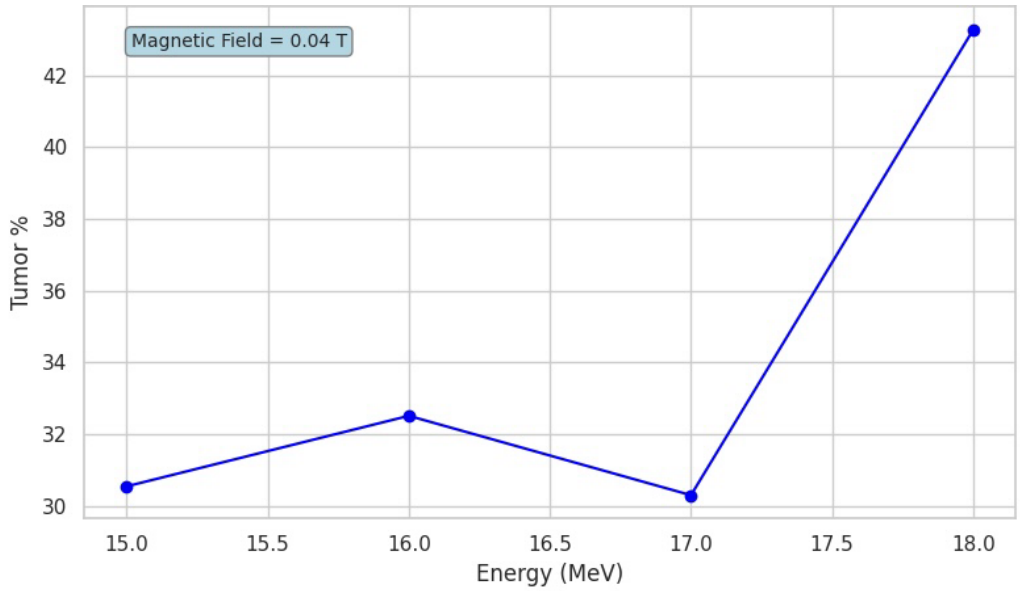

Figure 3.2: Electron Percentage energy deposit Deep tumor under 0.04 T magnetic field at various energies.

Table 3.2: Geant4-Simulated deflection of 10-electron beam in deep tumor under 0.06 T magnetic field at various energies.

Magnetic Field (T)	Energy (MeV)	PreTumor	Tumor	PostTumor	θ Mean (degree)	θ Std.Dev (degree)	Tumor %
0.06	15	20.9404	7.54592	0.272923	0.0040281	0.47815	26.23824278
0.06	16	20.0404	11.2453	1.79539	0.0113774	1.16594	33.99313626
0.06	17	20.2967	11.3222	3.44204	0.00806407	0.999863	32.29291628
0.06	18	20.3215	12.2241	4.32886	0.0153426	1.23781	33.15058715

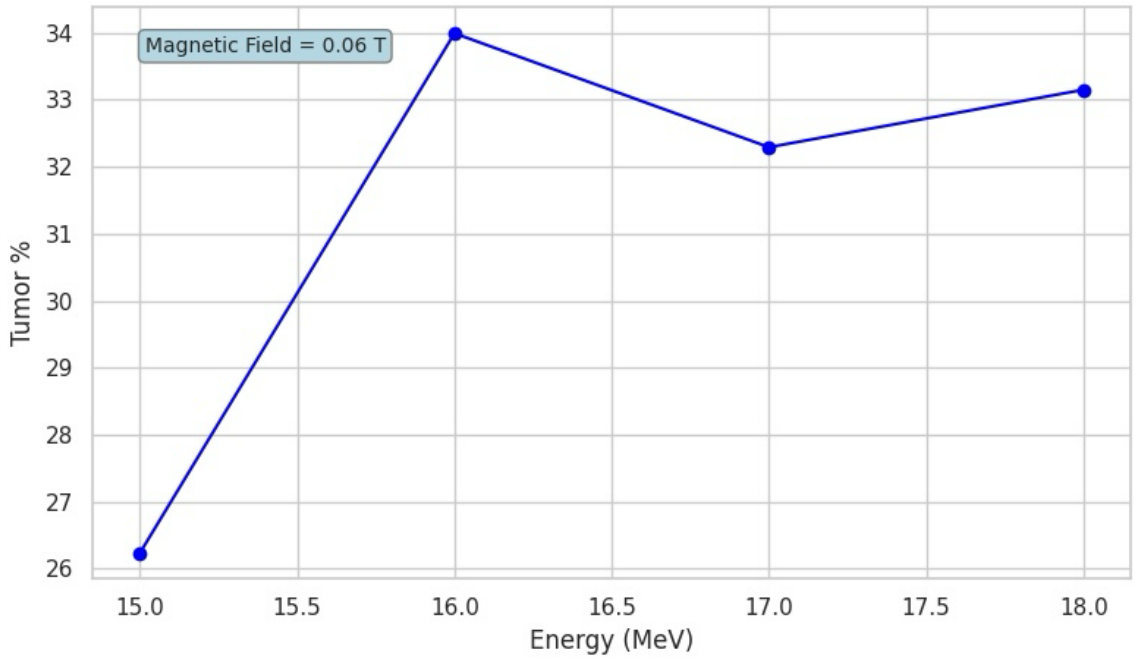

Figure 3.3: Percentage energy deposit Deep tumor under 0.06 T magnetic field at various energies.

Table 3.3: Geant4-Simulated deflection of 10-electron beam in deep tumor under 0.08 T magnetic field at various energies

Magnetic Field (T)	Energy (MeV)	PreTumor	Tumor	PostTumor	θ Mean (degree)	θ Std.Dev (degree)	Tumor %
0.08	15	22.8479	7.79772	1.332	0.0214548	1.64777	24.38492921
0.08	16	20.5327	11.3881	1.70517	0.00253194	0.440134	33.86697841
0.08	17	20.9449	11.7227	2.22706	0.00347442	0.453419	33.59453853
0.08	18	20.7288	12.0313	3.90168	0.00589509	0.756531	32.81700998

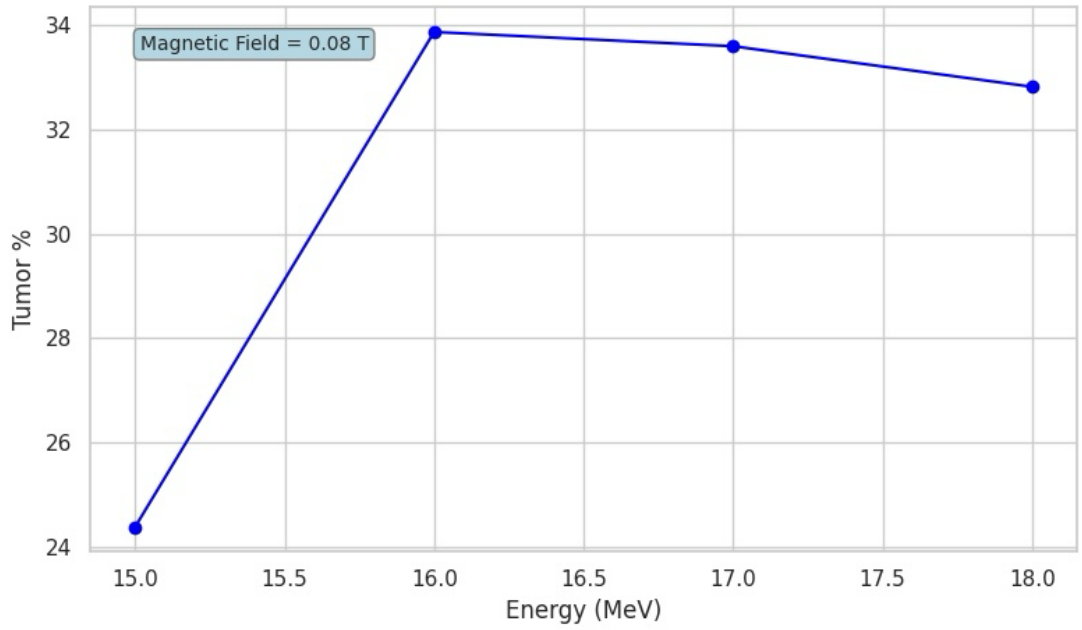

Figure 3.4: Percentage energy deposit Deep tumor under 0.08 T magnetic field at various energies.

The study examined how varying magnetic field strengths (0.04 T to 0.08 T) influence the percentage of energy deposited in deep-seated tumors at different electron beam energies (15 MeV to 18 MeV). The following trends were observed:

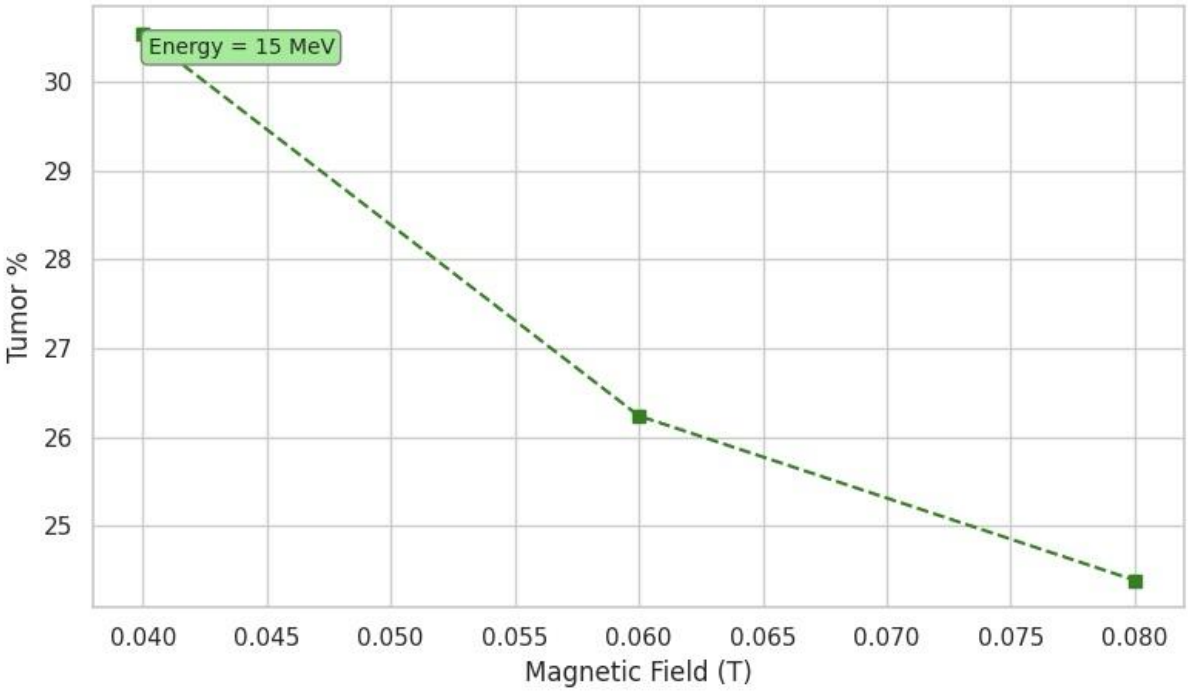

Figure 3.5: Percentage energy deposit Deep tumor under 15 MeV energy at various magnetic field.

The percentage of energy deposited decreases consistently with increasing magnetic field strength. This suggests that higher magnetic fields may deflect the electron beam away from the tumor target at this energy level.

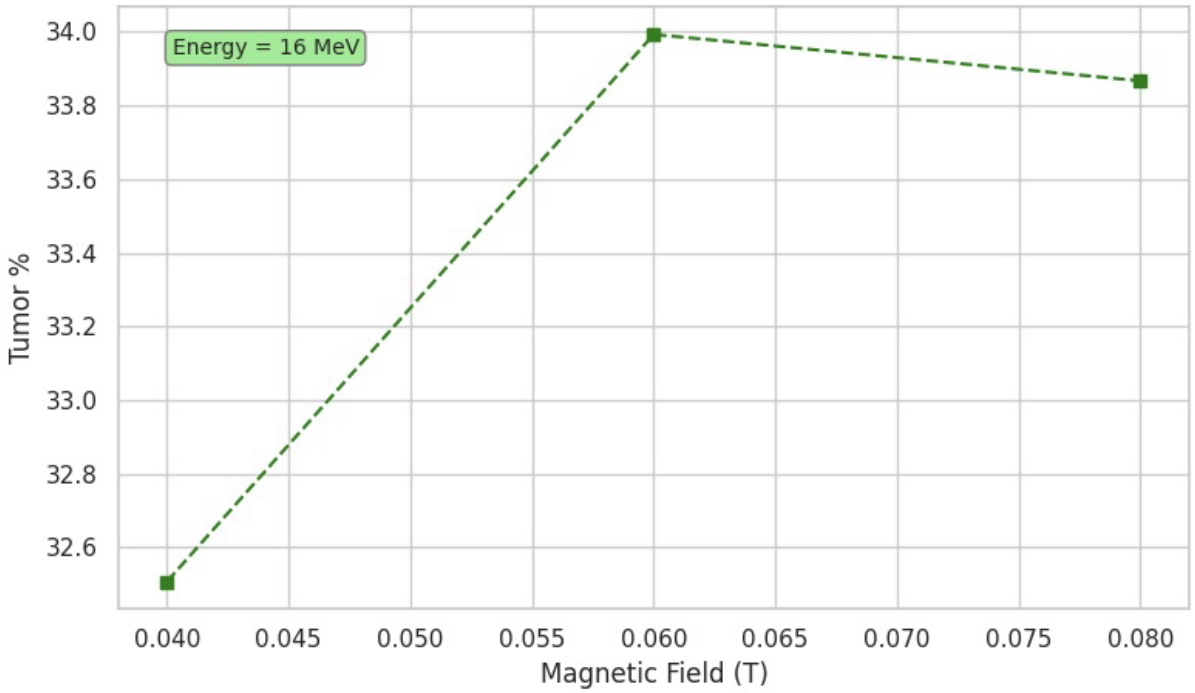

Figure 3.6: Percentage energy deposit Deep tumor under 16 MeV energy at various magnetic field.

Energy deposition initially increases with the magnetic field, peaking around 0.06 T, then slightly declines. This implies an optimal magnetic field strength near 0.06 T for maximizing energy delivery at 16 MeV.

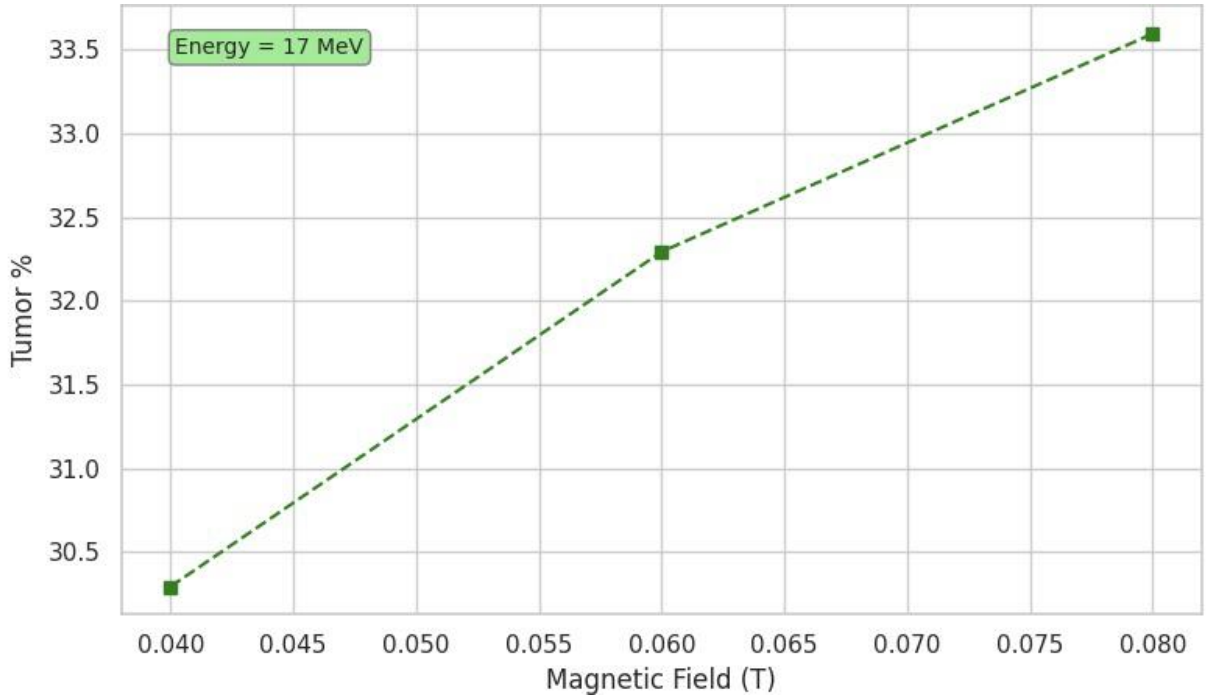

Figure 3.7: Percentage energy deposit Deep tumor under 17 MeV energy at various magnetic field.

A steady increase in tumor energy deposition is seen across the entire magnetic field range. This indicates a beneficial interaction between magnetic field and beam trajectory at this energy level.

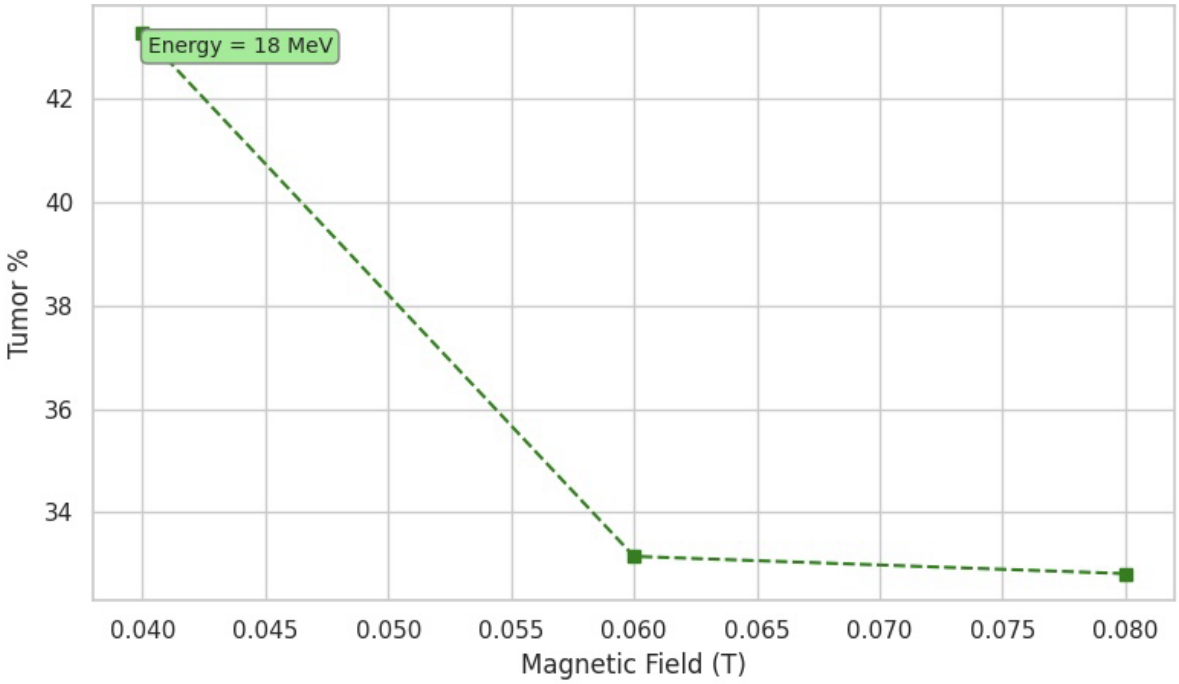

Figure 3.8: Percentage energy deposit Deep tumor under 18 MeV energy at various magnetic field.

A sharp decline in energy deposition is observed as the magnetic field increases, particularly beyond 0.04 T. This suggests that at higher beam energies, magnetic fields may significantly disrupt beam focus on the tumor.

Overall:

The interaction between magnetic field strength and beam energy demonstrates a non-linear behavior. Optimal energy deposition is dependent on carefully tuning both parameters. Specifically, energies around 16–17 MeV show the most promising outcomes for deep tumor targeting in the presence of magnetic fields, while too strong a magnetic field at lower (15 MeV) or higher (18 MeV) energies may reduce treatment efficacy.

The analysis of the deflection angle of electron beams across varying energies (15 to 18 MeV) at a deep tumor level under different magnetic field strengths (0.04 T, 0.06 T, and 0.08 T) reveals the following:

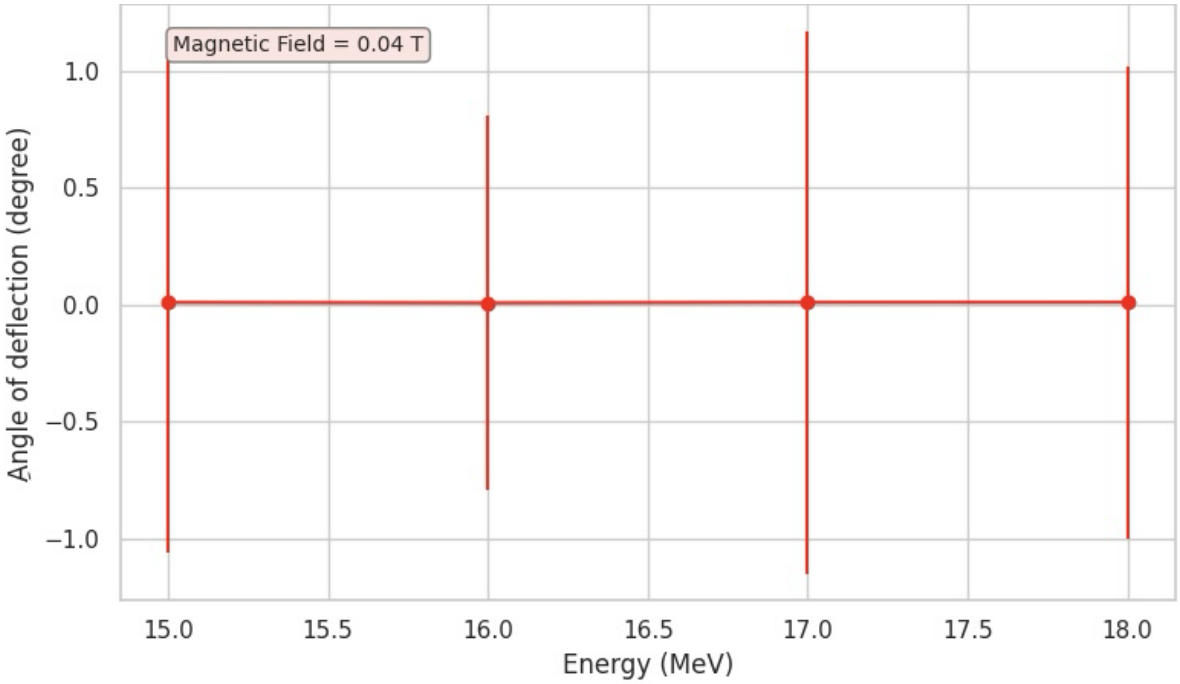

Figure 3.9: Angle of deflection versus electron beam energy in deep tumor region under 0.04 T magnetic field.

As shown in Figure 3.10, the electron beam experiences negligible angular deflection across the energy spectrum. The deflection remains close to zero degrees, indicating a minimal influence of the magnetic field at this strength in deep tissue.

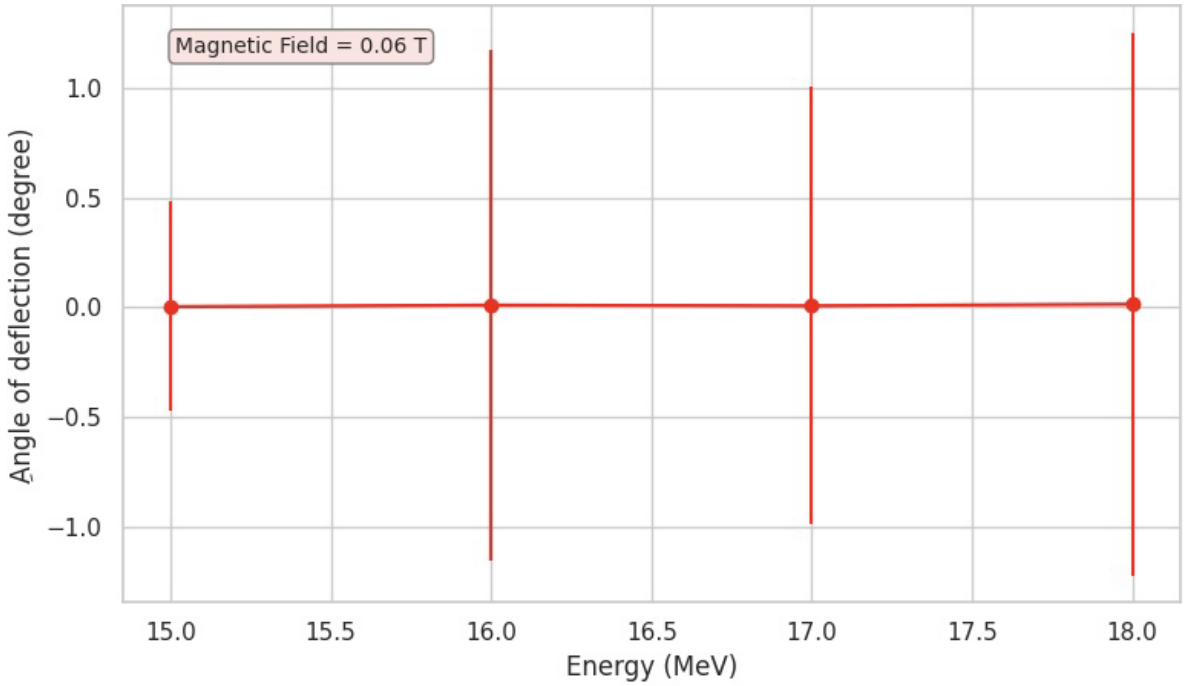

Figure 3.11: Angle of deflection versus electron beam energy in deep tumor region under 0.06 T magnetic field.

From Figure 3.12, a slight increase in angular deflection is observed, although the effect is still minor. The angular deflection does not exceed ±1°, indicating a mild but growing influence of the magnetic field on the electron path.

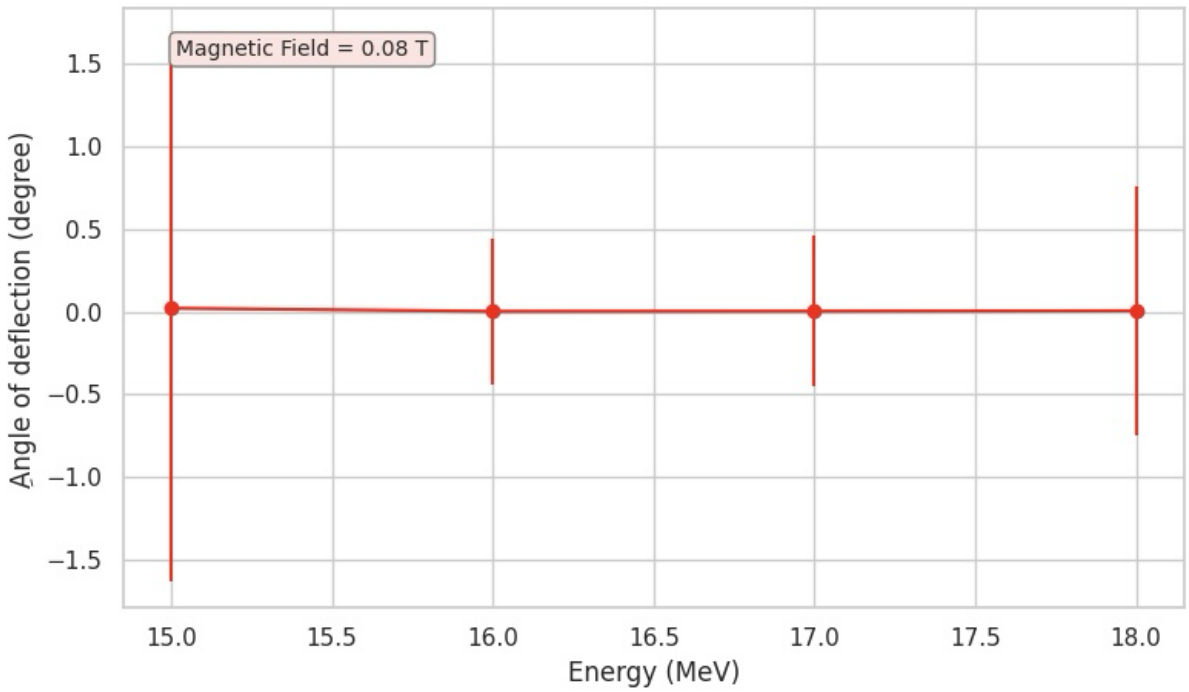

Figure 3.12: Angle of deflection versus electron beam energy in deep tumor region under 0.08 T magnetic field.

In Figure 3.12, the deflection becomes more pronounced, with angles approaching ±1.5° at the highest energy levels. This suggests that as the magnetic field strength increases, the Lorentz force acting on the electron beam becomes more significant, resulting in observable trajectory deviations even in deep-seated regions.

Overall:

The angle of deflection of electron beams in deep tumor regions increases with the strength of the magnetic field. However, due to the scattering and attenuation effects in deeper tissues, the magnitude of deflection remains relatively small even at higher magnetic field strengths. This outcome is crucial for designing magnetic field-assisted radiotherapy systems, as it confirms that moderate magnetic fields will not substantially alter beam direction in deep-seated tumors, preserving targeting accuracy while allowing for potential dose shaping or guidance in more superficial layers.

Shallow level :

Shallow radiation in electron beam therapy, we mean a high level of radiation given close to the surface.

Different energy levels were tested on shallow tumor in the presence of a constant magnetic field.

Table 3.4: Geant4-Simulation deflection of 10-electron beam in Shallow tumor under 0.04 T magnetic field at various energies.

Magnetic Field (T)	Energy (MeV)	PreTumor	Tumor	PostTumor	θ Mean (degree)	θ Std. Dev (degree)	Tumor %
0.04	8	9.28877	7.81445	0.158276	0.00680941	0.786422	45.27098926
0.04	9	8.40818	10.2171	0.723681	0.00261579	0.422181	52.80438572
0.04	10	7.81093	11.0093	2.02351	0.0170001	1.46943	52.81825622
0.04	11	8.1229	9.99713	4.75123	0.0081119	0.944365	43.71044709

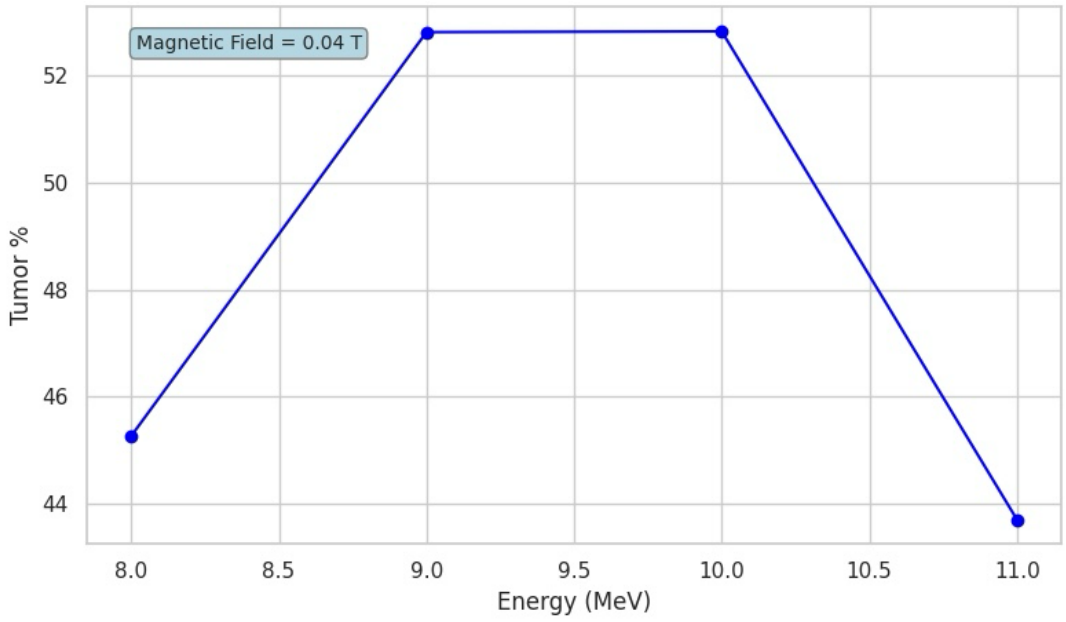

Figure 3.13: Percentage energy deposit shallow tumor under 0.04 T magnetic field at various energies.

Table 3.5: Geant4-Simulation deflection of 10-electron beam in Shallow tumor under 0.06 T magnetic field at various energies.

Magnetic Field (T)	Energy (MeV)	PreTumor	Tumor	PostTumor	θ Mean (degree)	θStd.Dev (degree)	Tumor %
0.06	8	10.6049	6.31735	0.19394	0.015506	1.31675	36.90862277
0.06	9	9.51218	8.95813	0.371014	0.00411633	0.467654	47.54511944
0.06	10	8.17954	11.0402	1.73013	0.0123027	1.36095	52.69817903
0.06	11	9.16641	9.17978	4.52225	0.0210429	1.68112	40.14169747

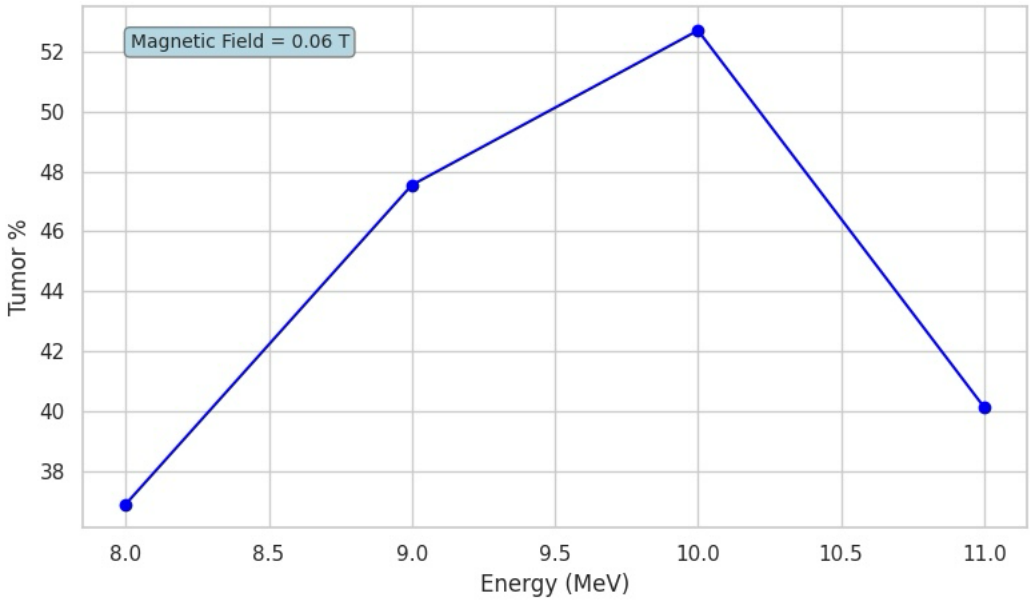

Figure 3.14:Percentage energy deposit shallow tumor under 0.06 T magnetic field at various energies

Table 3.6: Geant4-Simulation deflection of 10-electron beam in Shallow tumor under 0.08 T magnetic field at various energies.

Magnetic Field (T)	Energy (MeV)	PreTumor	Tumor	PostTumor	θ Mean (degree)	θ Std. Dev (degree)	Tumor %
0.08	8	11.1434	5.83253	0.0154019	0.00569125	0.868955	34.32650268
0.08	9	9.91011	9.09114	0.446717	0	0	46.74596579
0.08	10	8.23665	10.8874	1.60762	0.0115509	1.23409	52.51578865
0.08	11	10.1125	9.7218	3.66668	0.028321	1.83858	41.36763658

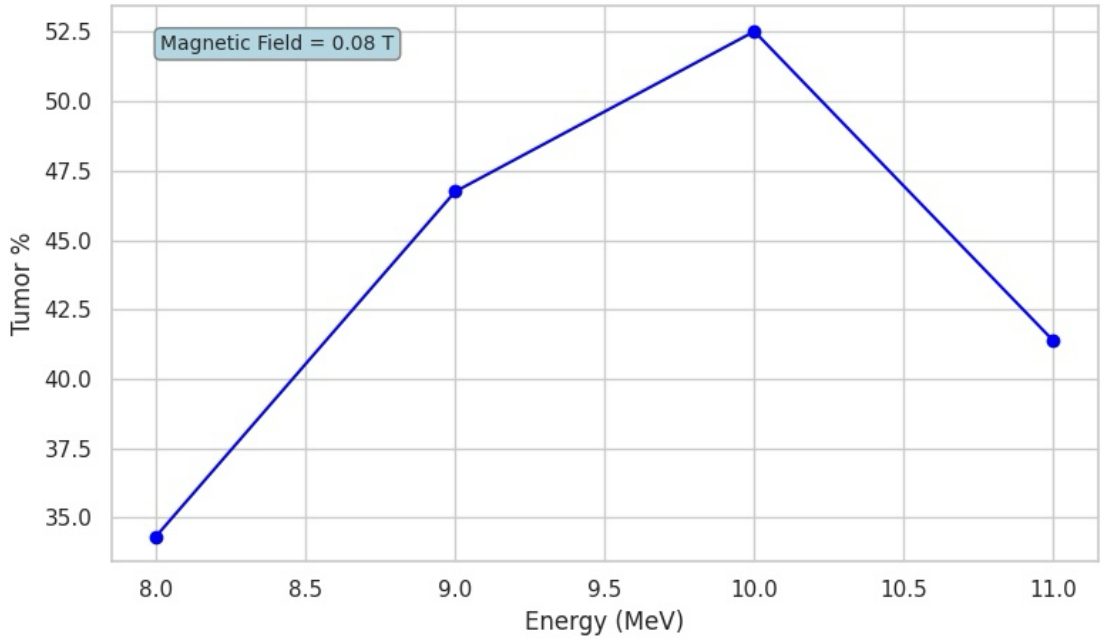

Figure 3.15:Percentage energy deposit shallow tumor under 0.08 T magnetic field at various energies

The results presented in Figures 3.16 through 3.19 demonstrate the behavior of electron beam energy deposition in shallow tumor regions across a range of magnetic field strengths. The key observations are as follows:

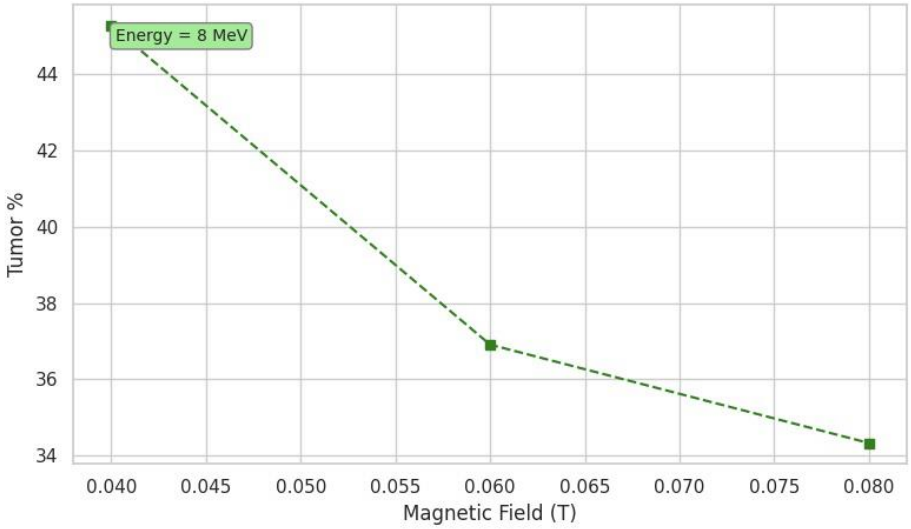

Figure 3.16:Percentage energy deposit Shallow Tumor under 8 MeV energy at Various magnetic field.

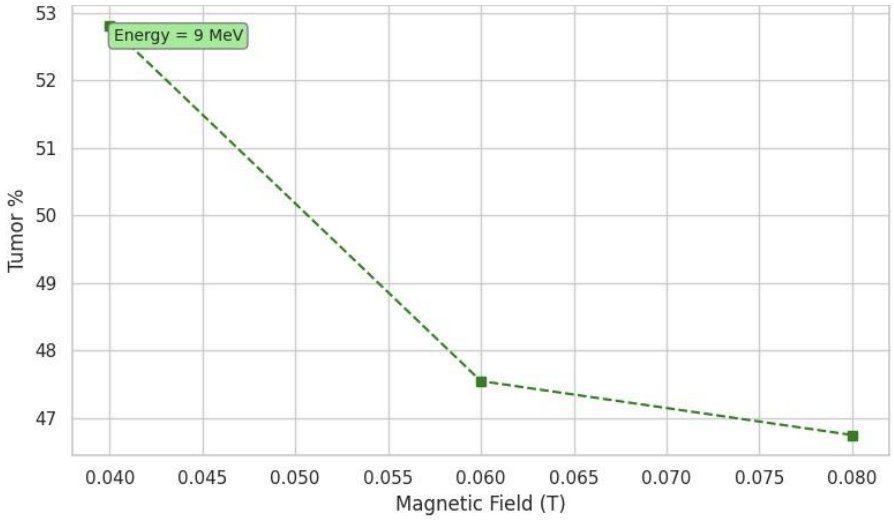

Figure 3.17:Percentage energy deposit Shallow Tumor under 9 MeV energy at Various magnetic field.

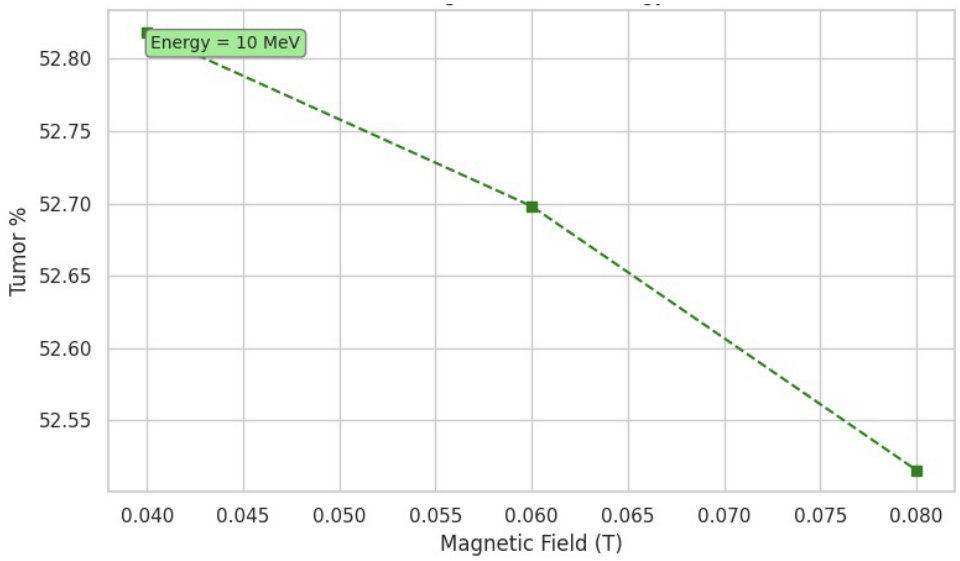

Figure 3.18:Percentage energy deposit Shallow Tumor under 10 MeV energy at Various magnetic field.

For electron energies of 8 MeV (Fig. 3.16), 9 MeV (Fig. 3.17), and 10 MeV (Fig. 3.18), there is a clear decreasing trend in tumor dose percentage as magnetic field strength increases from 0.04 T to 0.08 T. This indicates that stronger magnetic fields at these energy levels cause increased deflection or scattering, reducing beam concentration in the tumor volume and therefore lowering treatment efficiency.

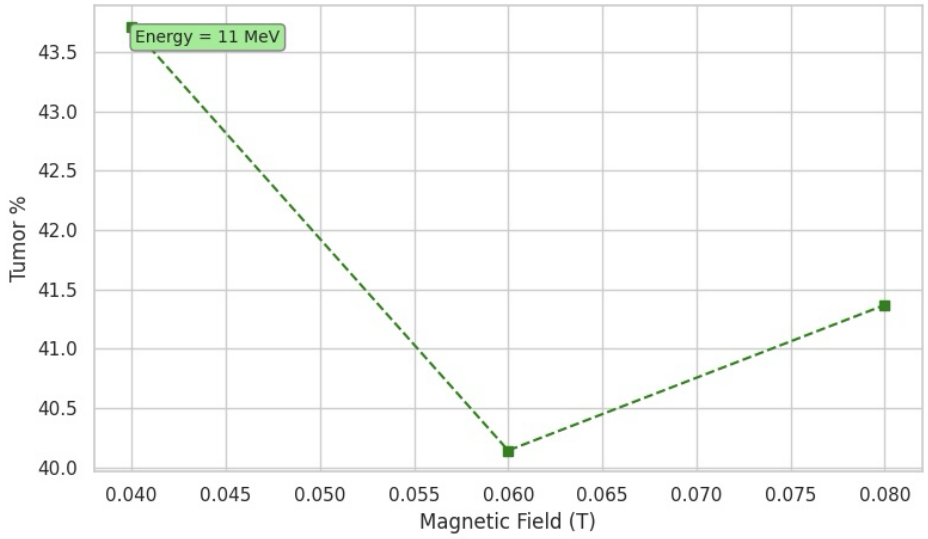

Figure 3.19:Percentage energy deposit Shallow Tumor under 9 MeV energy at Various magnetic field.

At 11 MeV, the energy deposition initially drops as magnetic field increases from 0.04 T to 0.06 T, but then slightly increases from 0.06 T to 0.08 T. This irregularity suggests that at higher beam energies, complex interactions between beam deflection and scattering may cause some redistribution of the dose, potentially returning some electrons into the tumor region.

Overall Conclusion:

Magnetic fields reduce the effectiveness of electron beam therapy in shallow tumor regions, particularly at lower energy levels. The deflection induced by magnetic fields decreases the percentage of energy deposited in the tumor, undermining the precision and efficiency of the treatment. Therefore, for optimal dose delivery in shallow tumor therapy, low-energy beams (8–10 MeV) should be used in conjunction with minimal or no magnetic field presence. Any use of magnetic steering in these contexts must be approached cautiously and only after careful modeling.

The angular deflection behavior of electron beams with energies ranging from 8 to 11 MeV was analyzed in a shallow tumor region under varying magnetic field strengths. The graphical data from Figures 3.20–3.22 reveal the following important trends:

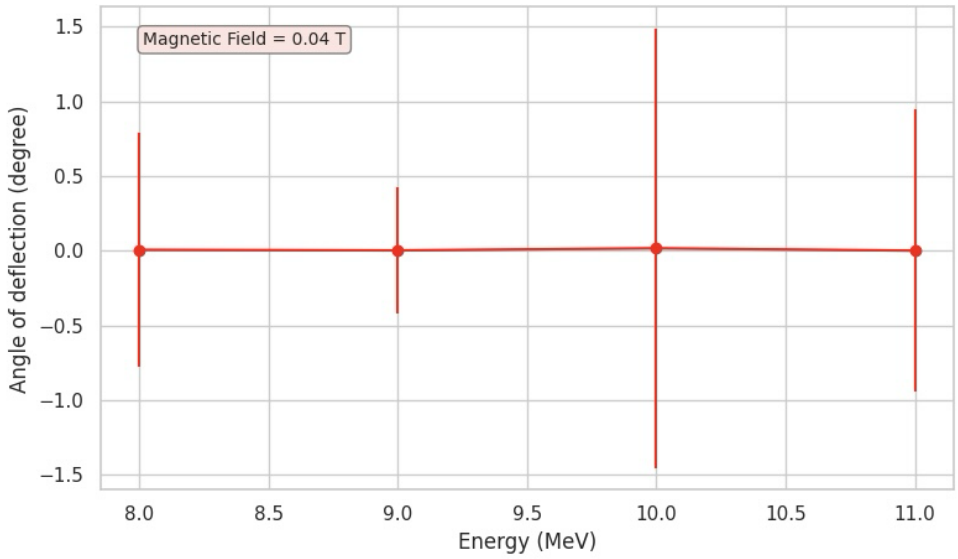

Figure 3.20:Angle of deflection versus electron beam energy in shallow tumor region under 0.04 T magnetic field

At the weakest magnetic field (0.04 T), the electron beam shows minimal angular deflection across all energy levels. The deflection angles remain close to zero degrees, and the standard deviation is small, indicating high beam stability and directionality, which is optimal for shallow tumor targeting.

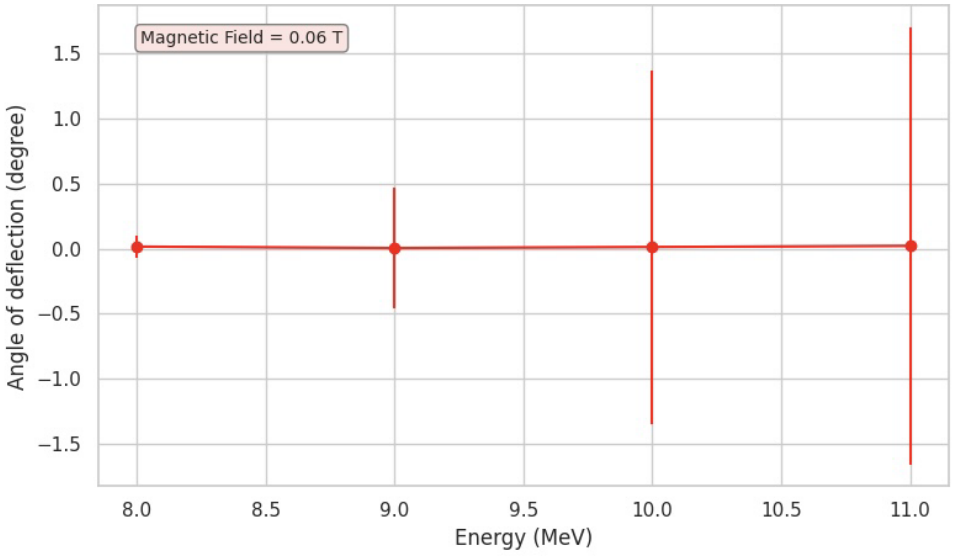

Figure 3.21:Angle of deflection versus electron beam energy in shallow tumor region under 0.06 T magnetic field

When the magnetic field strength is increased to 0.06 T, there is greater variability in the angle of deflection, particularly at higher energies. Although the average deflection angles remain low, the larger error bars suggest enhanced scattering or path deviation, which may lead to a broader or less focused dose distribution in the tumor region.

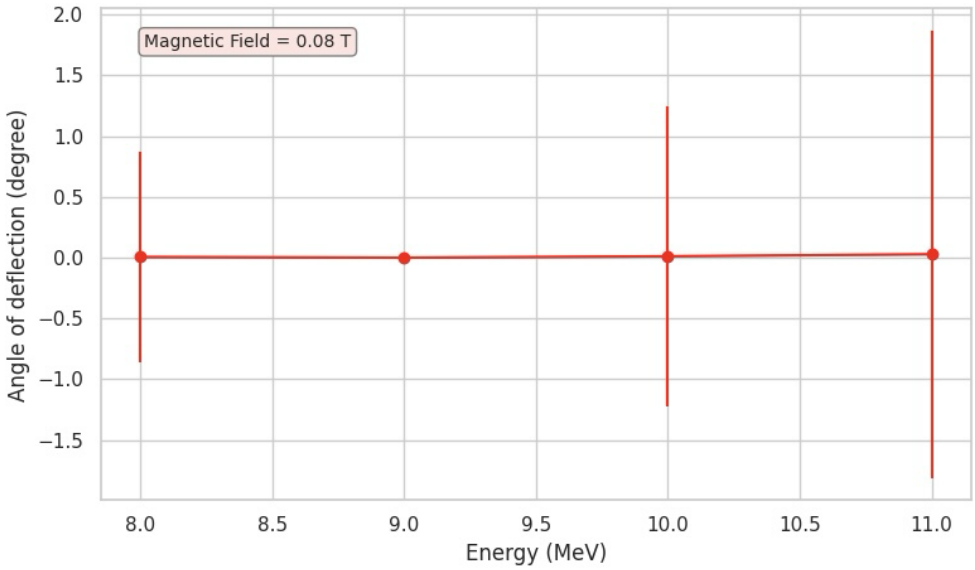

Figure 3.22:Angle of deflection versus electron beam energy in shallow tumor region under 0.08 T magnetic field

At 0.08 T, the angular deflection becomes even more inconsistent, with some deflections reaching nearly ±1.5°, especially at 10 and 11 MeV. The increased fluctuation implies that stronger magnetic fields significantly disturb the beam path, reducing the precision of energy delivery in shallow tumor therapy.

Overall:

In shallow tumor applications, increasing magnetic field strength results in greater angular deflection and instability of the electron beam. While the deflection angles themselves remain relatively small, the increased standard deviation highlights a loss of control over beam directionality. This may lead to suboptimal dose conformity and unintended exposure of healthy tissue. Therefore, for shallow tumor treatments, it is strongly recommended to use minimal magnetic field strengths (ideally ≤ 0.04 T) to ensure accurate targeting and minimal beam dispersion.

Chapter 4: Discussion

This study investigated the influence of magnetic fields on electron beam deflection and energy deposition in shallow and deep tumor regions using Geant4 simulations . It is a very reliable toolkit that helped in simulating the electron beam . Results show that the interaction between magnetic fields and charged particles significantly affects beam behavior and dose distribution:

For deep-seated tumors, higher beam energies (16–18 MeV) and moderate magnetic fields (0.06–0.08 T) improve beam focus and dose delivery.

In contrast, for shallow tumors, lower beam energies (8–10 MeV) combined with minimal magnetic field strength (0.04 T) minimize unwanted beam deflection and energy dispersion.

The findings emphasize the need for tailored treatment planning based on tumor depth, utilizing magnetic field adjustments to maximize therapeutic benefits while minimizing collateral damage to healthy tissues.

Consequently, it is recommended that radiation therapy protocols incorporate adjustable magnetic fields tailored to tumor depth in order to enhance dose targeting and ensure patient safety. Future treatment systems should be designed to support real-time modulation of magnetic field strength, particularly for cases involving tumors at varying depths. For effective treatment of deep tumors, electron beams with energies ≥16 MeV in conjunction with magnetic fields between 0.06 and 0.08 T are suggested to achieve optimal dose concentration and treatment accuracy. Conversely, for surface or shallow tumors, using 8–10 MeV electron beams while avoiding strong magnetic fields is advised to reduce beam deflection and preserve beam conformity. Additionally, the study recommends the use of anatomically realistic organ phantoms instead of generic water phantoms in electron beam research to more accurately replicate clinical treatment scenarios and improve the relevance of simulation outcomes.

References

[1] Kueng, R., Oborn, B. M., Roberts, N. F., Causer, T., Stampanoni, M. F., Manser, P., ... & Fix, M. K. (2020). Towards MR-guided electron therapy: Measurement and simulation of clinical electron beams in magnetic fields. Physica medica, 78, 83-92.

[2] Groeneveld, J. (2024). Monte Carlo studies in the applications of magnetic fields to electron radiotherapy (Master's thesis, University of Calgary, Calgary, Canada). Retrieved from https://prism.ucalgary.ca. https://hdl.handle.net/1880/117885

[3] Colmenares, R., Carrión-Marchante, R., Martín, M. E., Salinas Muñoz, L., García-Bermejo, M. L., Oller, J. C., Muñoz, A., Blanco, F., Rosado, J., Lozano, A. I., Álvarez, S., García-Vicente, F., & García, G. (2023). Dependence of Induced Biological Damage on the Energy Distribution and Intensity of Clinical Intra-Operative Radiotherapy Electron Beams. International Journal of Molecular Sciences, 24(13), 10816. https://doi.org/10.3390/ijms241310816

[4] Wideröe R. (1977). Elektronentherapie [Electron therapy]. Strahlentherapie, 153(3), 133–142.

[5] Vyas, V., Palmer, L., Mudge, R., Jiang, R., Fleck, A., Schaly, B., Osei, E., & Charland, P. (2013). On bolus for megavoltage photon and electron radiation therapy. Medical Dosimetry, 38(3), 268–273.

[6] Chu, J. C., Reiffel, L., Hsi, W. C & ,.Saxena, V. A. (2001). Modulation of radiotherapy photon beam intensity using magnetic field .International journal of cancer 96 ,Suppl.137–131 ,

[7] Ingalls, R. G. (2011, December). Introduction to simulation. In Proceedings of the 2011 winter simulation conference (WSC) (pp. 1374-1388). IEEE.

[8] Katsumura, Y., & Kudo, H. (2018). Interactions Between Radiation and Matter. Radiation Applications, 7-14.

[9] Boundless. (n.d.). Motion of a charged particle in a magnetic field. In Physics (Chapter 21.4). LibreTexts. https://phys.libretexts.org/Bookshelves/University_Physics/Physics_(Boundless)/21%3A_Magnetism/21.4%3A_Motion_of_a_Charged_Particle_in_a_Magnetic_Field.

[10] Caputo, M. V. (1984). *Stratigraphy, tectonics, paleoclimatology and paleogeography of northern basins of Brazil* [PhD dissertation, University of California].